Mutation of the PEBP-like domain of the mitoribosomal MrpL35/mL38 protein results in production of nascent chains with impaired capacity to assemble into OXPHOS complexes

Jodie M. Box, Jessica M. Anderson, and Rosemary A. Stuart*

Department of Biological Sciences, Marquette University, Milwaukee, WI 53233

ABSTRACT Located in the central protuberance region of the mitoribosome and mitospecific mL38 proteins display homology to PEBP (Phosphatidylethanolamine Binding Protein) proteins, a diverse family of proteins reported to bind anionic substrates/ligands and implicated in cellular signaling and differentiation pathways. In this study, we have performed a mutational analysis of the yeast mitoribosomal protein MrpL35/mL38 and demonstrate that mutation of the PEBP-invariant ligand binding residues Asp(D)232 and Arg(R)288 impacted MrpL35/mL38's ability to support OXPHOS-based growth of the cell. Furthermore, our data indicate these residues exist in a functionally important charged microenvironment, which also includes Asp(D)167 of MrpL35/mL38 and Arg(R)127 of the neighboring Mrp7/bL27m protein. We report that mutation of each of these charged residues resulted in a strong reduction in OXPHOS complex levels that was not attributed to a corresponding inhibition of the mitochondrial translation process. Rather, our findings indicate that a disconnect exists in these mutants between the processes of mitochondrial protein translation and the events required to ensure the competency and/or availability of the newly synthesized proteins to assemble into OXPHOS enzymes. Based on our findings, we postulate that the PEBP-homology domain of MrpL35/mL38, together with its partner Mrp7/bL27m, form a key regulatory region of the mitoribosome.

Monitoring Editor Karsten Weis ETH Zurich

Received: Apr 19, 2023 Revised: Sep 20, 2023 Accepted: Sep 25, 2023



SIGNIFICANCE STATEMENT

.edu).

- The functional significance of the conserved phosphatidylethanolamine binding protein (PEBP) domain found in all mitochondrial ribosomal mL38 protein family members, is currently unknown.
- Mutations of PEBP-invariant ligand binding residues in the yeast MrpL35/mL38 protein impact its
 ability to support OXPHOS-based cellular growth. The authors present evidence that mutations did
 not inhibit the process of mitoprotein synthesis but impacted the competency of resulting proteins
 to assemble into stable OXPHOS complexes.
- The findings suggest the mL38 proteins may serve to prime and regulate the mitoribosome, optimizing it to contribute to the posttranslational fate of newly synthesized proteins.

This article was published online ahead of print in MBoC in Press (http://www.molbiolcell.org/cgi/doi/10.1091/mbc.E23-04-0132) on October 4, 2023.

Conflict of interest: The authors declare that they have no conflict of interest. Author contributions: J.M.B. and R.A.S. conceived, coordinated the study, prepared all figures, and wrote the paper. J.M.B. completed all of the experiments shown. J.M.A. created the *mrp7* Arg(R)127 mutants and provided some preliminary which supported the development of the study. All data was analyzed with R.A.S. All authors reviewed the results and approved the final version of the manuscript.

*Address correspondence to: Rosemary A. Stuart (rosemary.stuart@marquette

Abbreviations used: COX, cytochrome c oxidase; Cytb, cytochrome b; hr, hour; min, minute; OXPHOS, oxidative phosphorylation; PE, phosphatidylethanolamine; PEBP, phosphatidylethanolamine binding protein; 5'FOA, 5-fluoroorotic acid.

© 2023 Box et al. This article is distributed by The American Society for Cell Biology under license from the author(s). Two months after publication it is available to the public under an Attribution–Noncommercial-Share Alike 4.0 International Creative Commons License (http://creativecommons.org/licenses/by-nc-sa/4.0). "ASCB®," "The American Society for Cell Biology," and "Molecular Biology of the Cell®" are registered trademarks of The American Society for Cell Biology.

INTRODUCTION

The mitochondrial oxidative phosphorylation (OXPHOS) enzymes are oligomeric complexes and mosaics in genetic origin. While the majority of the proteins that comprise the OXPHOS complexes are encoded by nuclear genes and synthesized on cytosolic ribosomes, the remainder, a small number of enzymatically key OXPHOS subunits, is encoded by the mitochondrial genome (the mtDNA). In the yeast Saccharomyces cerevisiae (S. cerevisiae), the mtDNA encoded OXPHOS subunits include cytochrome b (Cytb) of the cytochrome bc_1 enzyme, cytochrome c oxidase (COX) subunits 1, 2, and 3 (Cox1, Cox2, and Cox3, respectively) and subunits Atp6, Atp8, and Atp9 of the F₁F_o-ATP synthase (Borst and Grivell, 1978). These mtDNA encoded OXPHOS proteins are synthesized on mitochondrial ribosomes (mitoribosomes) within the mitochondrial matrix and are cotranslationally inserted into the inner membrane via the Oxa1 translocase (He and Fox, 1997; Hell et al., 1997, 1998, 2001; Jia et al., 2003, 2009; Gruschke et al., 2010; Haque et al., 2010; Ott and Herrmann, 2010; Itoh et al., 2021). Assembly of mitoribosomal synthesized proteins into the multisubunit OXPHOS complexes is favored when the process of mitochondrial protein synthesis is carefully coordinated with the availability of imported, nuclear encoded OXPHOS partner subunits, a process promoted in yeast when grown under respiratory-based conditions (Mick et al., 2011; Dennerlein and Rehling, 2015; Dennerlein et al., 2017; Anderson et al., 2022). Defects in the mitoribosome function (e.g., in overall translational capacity, fidelity, and/or rate of translation) can potentially lead to a reduction in the levels of nascent chains produced and/or in their competency to assemble into productive OXPHOS complexes. Newly synthesized mtDNA encoded proteins that fail to assemble into OXPHOS complexes are proteolytically turned over, a process favored under glucose fermentation growth in yeast. The expression of nuclear encoded OXPHOS partner subunits is largely repressed in the presence of glucose, whereas the process of mitochondrial translation still proceeds. Once uncoupled from OXPHOS assembly in this manner, the proteolytic turnover of the resulting mitoribosomal synthesized proteins is promoted (Anderson et al., 2022).

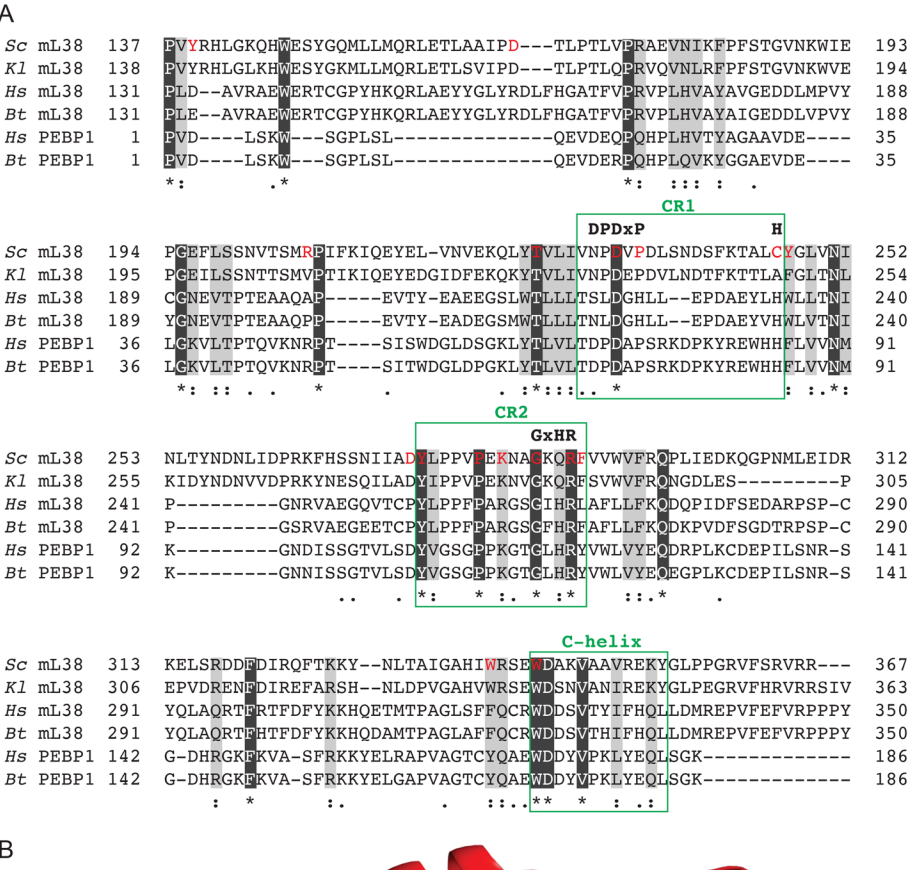
Mitoribosomes are distinct entities from their cytosolic counterparts, composed of rRNA (encoded by the mtDNA) and protein components, which, with the exception of one protein in the yeast S. cerevisiae, the Var1 protein, are encoded by nuclear genes. In accordance with the endosymbiotic origin of mitochondria, mitoribosomes evolved from bacterial ancestors. In addition to their evolutionarily conserved bacterial features, mitoribosomes have acquired novel protein features, so called "mitospecific" elements (novel proteins or domains/extensions on otherwise conserved proteins) not found in their bacterial relatives (Amunts et al., 2014, 2015; Brown et al., 2014, 2017; Greber et al., 2014; Desai et al., 2017; Santos et al., 2022). CryoEM analysis of mitoribosomes from several species have highlighted that the central protuberance (CP) and the membrane protuberance region represent areas of the large ribosomal subunit enriched in these mitospecific elements (Amunts et al., 2014; Brown et al., 2014).

Interfacing with the small ribosomal subunit, the mitoribosomal CP region also contains protein elements that extend to the peptidyl transferase center (PTC) of the ribosome, giving it the potential to influence intersubunit communication and/or the fidelity of the translational process. The CP is thus considered a key regulatory area of the mitoribosome, leading to the speculation that the mitospecific elements enriched in the CP may be molecularly involved in this regulation (Brown et al., 2014). The core architecture of the mitochondrial CP region is supported by the mitospecific mL38

protein and through interactions with other CP proteins (and mtRNA^{Val} or mtRNA^{Phe} in mammalian mitoribosomes) mL38 anchors the CP region to the rRNA core of the central structure of the large ribosomal subunit (Amunts et al., 2014; Brown et al., 2014; Greber et al., 2014; Chrzanowska-Lightowlers et al., 2017). In the yeast S. cerevisiae, the model organism of this study, the mitoribosomal CP region is composed of three mitospecific proteins MrpL35/mL38, MrpL28/mL40, MrpL17/mL46, and of proteins which have bacterial homologues but have evolved to contain C-terminal mitospecific extension sequences, such as the MrpL36/bL31m, MrpL7/uL5m, and Mrp7/bL27m proteins (Amunts et al., 2014; Box et al., 2017; Desai et al., 2017; Anderson et al., 2022). While the mL38, mL40, mL46, and bL27m proteins are common components of mitoribosomal CP structures across a diverse range of species, the mammalian mitoribosomes display several protein compositional differences from the fungal CP regions, including the presence of the MRPL58/ ICT1 (a peptidyl-tRNA hydrolase) protein, which physically partners the mL38 protein on the external surface of the mitoribosome (Richter et al., 2010; Brown et al., 2014; Aibara et al., 2020).

The mL38 mitoribosomal protein family forms a subgroup of a larger, diverse family of proteins known as the PEBP (Phosphatidylethanolamine Binding Protein) protein family, composed largely of nonmitochondrial, nonribosomal protein members (Serre et al., 1998, 2001; Tsoy and Mushegian, 2022; Susila and Purwestri, 2023). PEBP proteins are found in many bacteria, archaea and broadly in eukaryotes, and include proteins such as the Raf-kinase inhibitor protein (RKIP) in mammals, and the flowering locus T (FT) protein in plants (Banfield and Brady, 2000; Chautard et al., 2004; Faure et al., 2007; Shemon et al., 2010). Involved in diverse cell signaling pathways, often underpinning cellular proliferation and differentiation events, the PEBP proteins were originally named for their proposed ability to bind the lipid phosphatidylethanolamine (PE) in vitro. The functional relevance of binding of PE has not been demonstrated for any PEBP family member to date however (Tsoy and Mushegian, 2022). Rather, the PEBP proteins broadly have been proposed to be involved in small molecule metabolism, functioning possibly in the production, conjugation and/or removal of small anionic ligand metabolites (Tsoy and Mushegian, 2022). Crystal structures of PEBP proteins from plants and mammalian sources indicate that PEBP family members share a largely β -fold conformation with a conserved small cavity, a charged ligand binding pocket, close to the surface of the protein (Serre et al., 1998, 2001; Banfield and Brady, 2000; Tsoy and Mushegian, 2022). CryoEM analyses of yeast and mammalian mitoribosomes have indicated the characteristic PEBP β-fold conformation is a conserved feature among the mitoribosomal mL38 family members (Amunts et al., 2014, 2015; Brown et al., 2014). The PEBP domain of the mL38 proteins is exposed to the external surface of the mitoribosome, raising the possibility that it may form a binding site within the mitoribosomal CP region for external ligands or metabolite signaling molecules. Initial evidence for the potential importance of the PEBP domain in the mL38 protein family was provided with the isolation of a temperature sensitive yeast MrpL35/mL38 mutant harboring a mutation in a highly conserved residue within the PEBP domain (Tyr[Y]275 of MrpL35/ mL38; Box et al., 2017).

In this present study we have adopted a mutational approach to explore the importance of putative ligand-binding domain residues and other conserved residues within the PEBP-homology domain for the function of the *S. cerevisiae* MrpL35/mL38 protein. Our findings demonstrate the functional importance of the putative ligand-binding pocket for MrpL35/mL38's ability to support respiratory



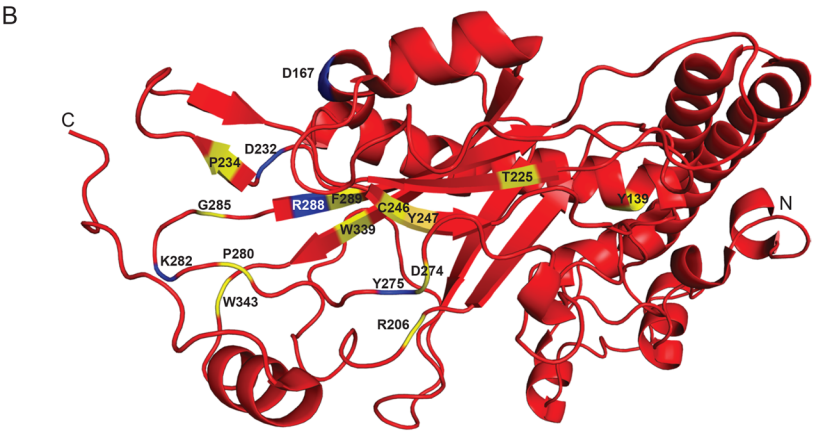


FIGURE 1: Identification and mutation of mL38/PEBP conserved residues in MrpL35/mL38. A) Multiple sequence alignment of select mL38 and PEBP family members was performed with CLUSTAL O, with amino acid residue numbers indicated. Sequences used and their UniProt identifiers are: Sc mL38, S. cerevisiae MRPL35/mL38 [Q06678], Kl mL38, Kluyveromyces lactis MRPL35/mL38 [A0A5P2UAF8]; Hs mL38, Homo sapiens (human) MRPL38/mL38 [Q96DV4]; Bt mL38, Bos taurus (bovine) MRPL38/mL38, [Q3ZBF3]; Hs PEBP1, human PEBP1 [P30086]; Bt PEBP1 bovine PEBP1 [P13696]. Residues corresponding to the bovine PEBP1 CR1 and CR2 regions with their conserved DPDxP.H and GxHR motifs, respectively, and the C-helix region, are indicated by boxes. Black-shaded, white-type represent residues conserved (*) among all proteins analyzed, while gray-shaded area indicates conservation between groups of residues with strongly similar properties (as indicated by the CLUSTAL symbol ":"). The CLUSTAL "." symbol indicates conservation between residues of weakly similar properties. Residues in red type in the Sc mL38 sequence indicate those targeted for mutagenesis. B) PyMol image of S. cerevisiae MrpL35/mL38 protein (from PDB 5MRC), with residues targeted for mutagenesis indicated in yellow (nonphenotypic) and blue (phenotypic).

growth and highlight a close relationship between MrpL35/mL38 and the C-terminal mitospecific domain of Mrp7/bL27m in this respect. While mutation of conserved features of the PEBP-homology domain did not inhibit MrpL35/mL38's support of the mitoribosomal protein synthesis process, it did result in reduced levels of OXPHOS assembly and hence compromised respiratory-based growth capacity of the cell. Our findings here indicate that the MrpL35/mL38, together with its partner protein Mrp7/bL27m, play an influential role in ensuring that the mitotranslational process is optimized to yield newly synthesized proteins competent for productive assembly into functional OXPHOS enzymes.

RESULTS

Identification of PEBP-invariant residues as important for the function of MrpL35/mL38

To gain a greater insight into the PEBP-homology domain of the mL38 proteins, we initially performed a sequence alignment of the S. cerevisiae MrpL35/mL38 protein and representative members of the mL38 protein family and two conserved nonmitochondrial and nonribosomal PEBP protein family members (Figure 1A). Structural analysis of several classical (i.e., nonmitoribosomal) PEBP proteins, have demonstrated that the PEBP ligand binding pocket is surface exposed and formed by the C-terminal helix domain (C-helix) and two strand-connecting regions termed CR1 and CR2, regions of notable sequence conservation amongst PEBP family members (Figure 1A). Furthermore, the PEBP ligand binding pocket has been reported to contain five "nearly invariant" polar residues, highly conserved throughout members of the PEBP protein family (Serre et al., 1998, 2001; Tsoy and Mushegian, 2022). Following the bovine PEPB1 protein numbering, these nearly invariant polar residues correspond to Asp(D)69, Asp(D)71, His(H)85, His(H)117, and Arg(R)118 (Figure 1A; Supplemental Table S1). Evolutionary substitutions in these residues are considered exceedingly rare among PEBP proteins but have been noted to occur in the clade of mL38 family members (Tsoy and Mushegian, 2022). For example, PEBP nearly invariant residues His(H)85 and His(H)117 are not found in the fungal MrpL35/mL38 proteins analyzed yet are conserved in the mammalian mL38 proteins. A cysteine residue (Cys[C]246) and glutamine (Gln[Q]287) are present at these locations in the S. cerevisiae MrpL35/mL38 instead. PEBP nearly invariant residue Asp(D)69 is not conserved among the mito-

chondrial mL38 members, being replaced by an asparagine residue Asn(N)230 in S. cerevisiae MrpL35/mL38. The remaining two nearly invariant PEBP residues, Asp(D)71 and Arg(R)118 (bovine PEBP1 numbering) however are fully conserved among the mL38 family members analyzed and they correspond to residues Asp(D)232 and Arg(R)288 of S. cerevisiae MrpL35/mL38 (Figure 1A; Supplemental Table S1). In addition, a number of apolar residues neighboring the PEBP-signature invariant polar residues are also characteristically conserved among PEBP members and include (bovine PEBP1 numbering) Pro(P)70, Pro(P)73, and Gly(G)115 (Serre et al., 1998, 2001; Banfield and Brady, 2000; Tsoy and Mushegian, 2022). These residues are conserved also among the fungal MrpL35/mL38 proteins analyzed, where they correspond to Pro(P)231, Pro(P)234, and Gly(G)285 of MrpL35/mL38, respectively. The mL38/PEBP sequence alignment also revealed several other residues highly conserved among the mL38/PEBP proteins analyzed (Figure 1A). These residues (using S. cerevisiae MrpL35/mL38 numbering) include Thr(T)225, located immediately N-terminal to the CR1 region and residues Tyr(Y)275, Pro(P)280, and Lys(K)282 within the CR2 region. Sequence conservation among the PEBP/mL38 proteins was also observed in the "C-helix" region, and includes residues Trp(W)339, Trp(W)343, Asp(D)344, and Val(V)347 of S. cerevisiae MrpL35/mL38 (Figure 1A). The C-helix region has been proposed to "gate" access to the ligand-binding pocket of PEBP proteins and the sequence conservation highlights the potential importance of this region for the mL38 proteins (Serre et al., 1998).

To probe the functional relevance of the PEBP-like domain in MrpL35/mL38, several of the identified conserved residues were targeted for PCR-based site-directed mutagenesis (Figure 1B; Supplemental Table S1). Selected residues were individually mutated to Ala(A) and the resulting mrpL35 mutant derivatives were analyzed for their ability to complement the $\Delta mrpL35$ yeast mutant, that is, to support aerobic-based growth on the nonfermentable carbon source, glycerol (Figure 2A; Supplemental Figure S1). The presence of MrpL35/mL38 is essential for mitoribosomal translation and hence for respiratory-based growth (Box et al., 2017; Zeng et al., 2018). Individual mutation of MrpL35 residues Tyr(Y)139, Arg(R)206, Thr(T)225, Pro(P)234, Cys(C)246, Tyr(Y)247, Asp(D)274, Pro(P)280, Gly(G)285, Phe(F)289, Trp(W)339, and Trp(W)343 in this manner had no major deleterious impact on MrpL35/mL38's ability to support aerobic-based metabolism, both at 30°C (optimal growth temperature for yeast) and under the temperature stress conditions of 37°C (Supplemental Figure S1, A-F; Supplemental Table S1). Moreover, double mutants mrpL35P234A;C246A and mrpL35C246A;G285A also displayed no discernable growth phenotype, further demonstrating the nonessential nature of conserved residues Pro(P)234, Cys(C)246, and Gly(G)285 for MrpL35/mL38's function (Supplemental Figure S1F; Supplemental Table S1). The absence of a discernable growth phenotype in these mrpL35 mutants indicates that these residues are not essential for the function of MrpL35/mL38.

In contrast, mutation of the CR2 conserved residue Lys(K)282 to Ala(A), that is, *mrpL35*^{K282A}, resulted in a modest respiratory growth defect at the elevated temperature of 37°C (Supplemental Figure S1C). However, the *mrpL35*^{D232A} and *mrpL35*^{R28BA} mutants, bearing individual mutation of the two PEBP nearly invariant, polar residues conserved in the mL38 family, that is, Asp(D)232 and Arg(R)288 of MrpL35/mL38, resulted in an impaired OXPHOS-based growth at 37°C (Figure 2A). Growth of the *mrpL35*^{D232A} and *mrpL35*^{R28BA} mutants, however, was somewhat better than the previously characterized temperature sensitive *mrpL35*^{Y275A} mutant (Box et al., 2017) analyzed in parallel. The double mutant *mrpL35*^{D232A,R28BA}, where both D232 and R288 residues were mutated in the same MrpL35/mL38 protein, exhibited a strong respiratory growth defect at 37°C, indicating that having no charged residues in positions 232 and 288 of MrpL35/mL38 was more deleterious than retaining one or other

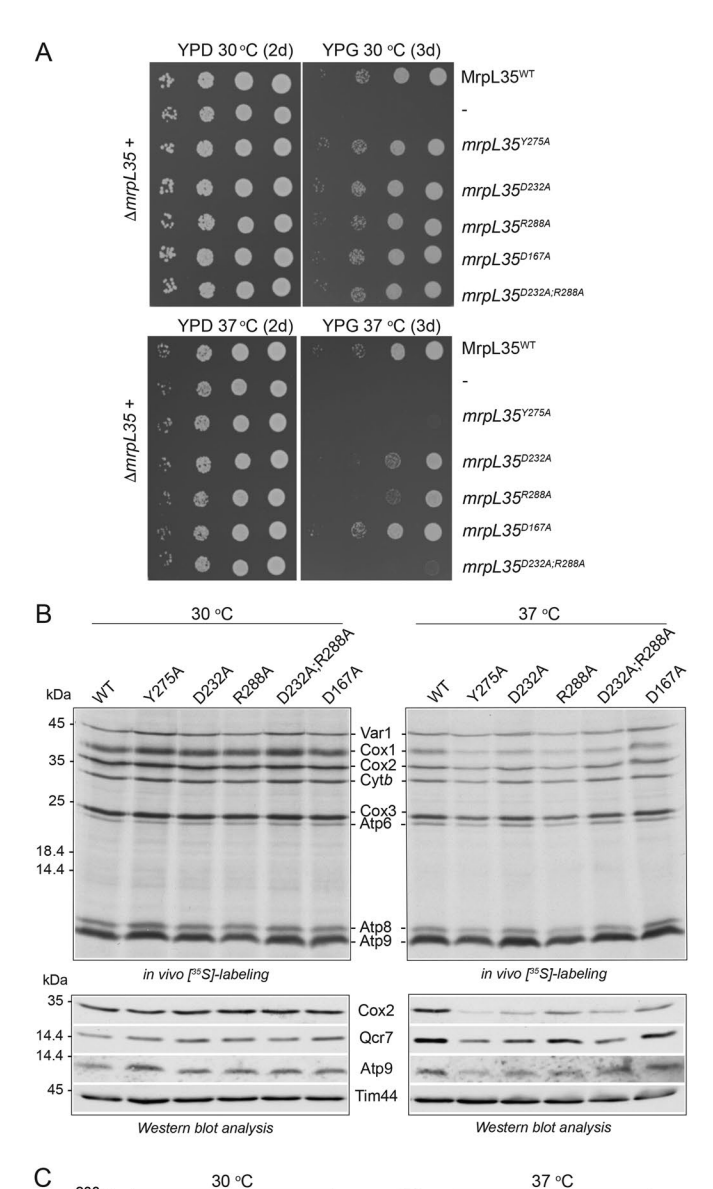
of them (Figure 2A). Given that the mutation of residues Asp(D)232 and Arg(R)288 yielded the strongest impact on MrpL35/mL38's ability to support aerobic-based growth, we focused our next efforts on exploring functional consequences of these two mutations for cellular OXPHOS capacity and did not further pursue the analysis of the other *mrpL35* mutants at this stage.

Mitochondrial translation and OXPHOS assembly are uncoordinated in mrpL35 Asp(D)232 and Arg(R)288 mutants

To ascertain whether the Ala(A) mutation of residues Asp(D)232 and/ or Arg(R)288 directly impacted MrpL35/mL38's ability to support mitochondrial translation per se, we analyzed mitoribosomal activity in these mrpL35 mutants. Mitochondrial protein synthesis was monitored in mutant cells grown in galactose (an OXPHOS nonrepressible fermentable carbon source) at the permissive (30°C) or stress temperatures (37°C), using an in vivo [35S]methionine-radiolabeling approach (in the presence of cycloheximide to inhibit cytoplasmic protein synthesis; Figure 2, B, upper panels and C). The mitotranslational behavior (level and profile of newly synthesized proteins) of the single and double Ala(A) exchange mutants, that is, mrpL35D232A, mrpL35^{R288A}, and mrpL35^{D232A,R288A}, respectively, were compared with the previously published mrpL35Y275A mutant and wild-type (WT) MrpL35/mL38 control. Mitochondrial translation activity levels were similar in all mrpL35 mutants relative to the WT control when monitored at the permissive temperature of 30°C (Figure 2, B, upper left panel and C). At the nonpermissive growth temperature of 37°C, the mrpL35 mutants all retained their capacity to support mitotranslation, as robust mitochondrial protein synthesis was recorded in each of the *mrpL35* mutants (Figure 2, B, upper right panel and C). A partial reduction of the level of total protein synthesis was recorded in the mrpL35R288A mutant, similar to that observed for the mrpL35Y275A mutant, however the mitotranslation activities of the mrpL35^{D232A} and double mutant mrpL35^{D232A,R288A}, resembled those of the WT MrpL35/mL38 control (Figure 2C). Despite their retained capacity for mitochondrial translation when grown at 37°C, a reduction cellular OXPHOS complex levels, COX (as indicated by steady state levels of Cox2 subunit), cytochrome bc_1 (as indicated by Qcr7 levels), and of the F₁F₀-ATP synthase (Atp9 levels), was observed in each of the mrpL35 mutants (Figure 2B, right lower panel; Supplemental Figure S2A). The OXPHOS complex levels were the least impacted in the mrpL35R288A mutant, despite its observed partial reduction in mitotranslation output displayed at 37°C. A more pronounced decrease in OXPHOS subunits was observed in both the mrpL35D232A and mrpL35D232A,R288A mutants, where no decrease in translational outputs was observed at the elevated temperature. The levels of OXPHOS subunits were not adversely affected in the mutants when grown at the permissive temperature of 30°C (Figure 2B, lower left panel).

Given the potential importance of the charged PEBP-invariant Asp(D)232 and Arg(R)288 residues for supporting MrpL35/mL38's function, we next mutated these residues (individually at first) to ones of opposite charge. Asp(D)232 was changed to an Arg(R) residue, and Arg(R)288 mutated to Asp(D). Growth of the resulting yeast strains harboring the $mrpL35^{D232R}$ and $mrpL35^{R288D}$ derivatives appeared normal at 30°C on fermentable and nonfermentable (respiratory) media (Figure 3A). A strong temperature-sensitive respiratory growth defect was however observed with the charge reverse mrpL35 mutants when grown at 37°C, and they resembled the previously reported $mrpL35^{Y275D}$ mutant analyzed in parallel (Figure 3A).

In vivo radiolabeling indicated that when cultivated in galactose at 30°C, the overall levels of mitotranslation in the *mrpL35* mutant cells were somewhat elevated relative to the WT control cells, in



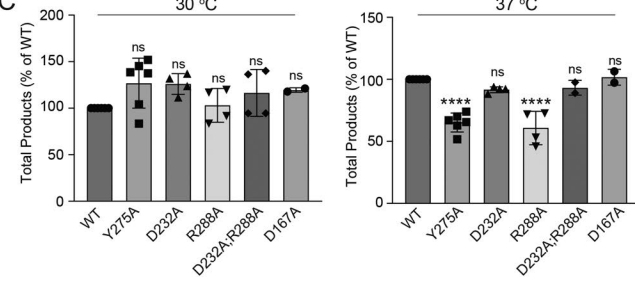


FIGURE 2: Mutation of charged residues Asp(D)232 and Arg(R)288 to neutral Ala(A) disturbs MrpL35/mL38's ability to support assembly of OXPHOS complexes. A) 10-fold serial dilutions (dilutions from right to left) of $\Delta mrpL35$ strains with pRS413 plasmid containing no insert (-), or a gene insert encoding the WT MrpL35/mL38 protein (MrpL35^{WT}) or a mutated mrpL35 derivative, as indicated. Strains were taken from 24 h growths on selective SD plates and spotted onto YP plates containing either glucose (YPD; 2d) or glycerol (YPG; 3d) and incubated at either 30 or 37°C. B and C) Indicated mrpL35 strains adapted to galactose selective synthetic media were grown at 30 or 37°C to mid-log phase, as described in Materials and Methods. B) Mitochondrial translation capacity was analyzed in vivo for 10 min in the presence of cycloheximide and [35S]methionine. Cells were isolated, solubilized, and newly synthesized proteins were analyzed by

particular for the in the mrpL35^{D232R} and mrpL35^{Y275D} mutants where a significant increase was measured (Figure 3, B, left upper panel and C). In contrast when grown at 37°C, the level of all proteins (with the exception of Var1) synthesized by the mitoribosomes was somewhat reduced in the mrpL35D232R and mrpL35Y275D mutants (Figure 3, B, right upper panel and C). The levels of mitoribosomal translation in the mrpL35R288D mutant grown at both 30 and 37°C however, more resembled that of the WT MrpL35/mL38 control, indicating the impact of the mutation of residues of Asp(D)232 and Arg(R)288 of MrpL35/mL38 did not produce a uniform phenotypic result on the mitoribosomal capacity for protein synthesis.

Cellular steady state levels of the OXPHOS complex subunits analyzed in the mrpL35D232R and mrpL35R288D mutant cells grown at 30°C appeared similar to the WT MrpL35/mL38 control (Figure 3B, lower panels). Mitochondria isolated from the mutants grown at this permissive temperature displayed normal levels of cytochrome bc1 (complex III) and F₁F₀-ATP synthase (complex V) and somewhat reduced levels (in particular in the mrpL35^{D232R} mutant) of COX (complex IV), as indicated by BN-PAGE analysis (Supplemental Figure S3). An altered ratio of the III₂-IV₂:III₂-IV₁ supercomplex forms were observed in the mutants (especially in the mrpL35D232R mutant) when the analysis was performed with digitonin solubilized mitochondrial extracts (Supplemental Figure S3A). The reduction in III₂-IV₂ species can be attributed to decreased complex IV levels relative to complex III levels and observed when solubilization in dodecylmaltoside (DDM) is performed, a detergent that separates complex III from IV enabling their individual analysis (Supplemental Figure S3B). The observed reduction of COX levels in the $mrpL35^{D232R}$ mutant at the permissive temperature and in contrast to the other OXPHOS complexes analyzed suggests that COX assembly was more susceptible to the defect(s) caused by the mrpL35 mutations, as previously observed for the Tyr(Y)275 mutations of MrpL35/mL38 (Box et al., 2017). When grown at 37°C, a strong reduction in cellular content of all OXPHOS complexes analyzed, that is, cytochrome bc₁, COX and F₁F_o-ATP synthase levels (as judged by Cox2, Qcr7 and Atp9 levels) was observed in each of the mrpL35 mutants,

SDS-PAGE and Western blotting, followed by autoradiography (upper panels). The equivalent of OD_{600} 0.3 of cells were loaded on each gel. Steady state levels of OXPHOS proteins Cox2, Qcr7, and Atp9, and Tim44 (loading control) from these cell extracts were also analyzed by Western blotting and immunedecoration with indicated antibodies (lower panels). Note the exposure times for the OXPHOS subunit decorations in the 37°C samples were approximately twice that used for the 30°C samples, as OXPHOS assembly, in particular the COX complex, is generally reduced in 37°C grown cells. The data from independent Western blots were quantified and summarized in Supplemental Figure S2A. C) The total amount of proteins synthesized during the in vivo radiolabeling period for each yeast strain in B) (i.e., sum of Var1, Cox1, Cox2, Cox3, Cytb, Atp6, Atp8, and Atp9 synthesis signals) was quantified by phosphorimaging or ImageJ analysis of resulting autoradiographs. Data from independent experiments and autoradiographs (n = 2-6) are provided, as indicated. The total product sum was expressed as a percentage of WT MrpL35/ mL38 WT control for each temperature. The significance between measurements was determined by one-way ANOVA using GraphPad Prism 9. Comparison of each mrpL35 mutant to its respective WT control, resulted in either no significant difference (ns), or in a significant difference and as indicated by ****, p < 0.0001; Abbreviations: WT MrpL35/mL38; Y275A, mrpL35^{Y275A}, D232A, mrpL35^{D232A}; R288A, mrpL35^{R288A}; D232A;R288A, mrpL35^{D232A;R288A}; D167A, and mrpL35^{D167A}.

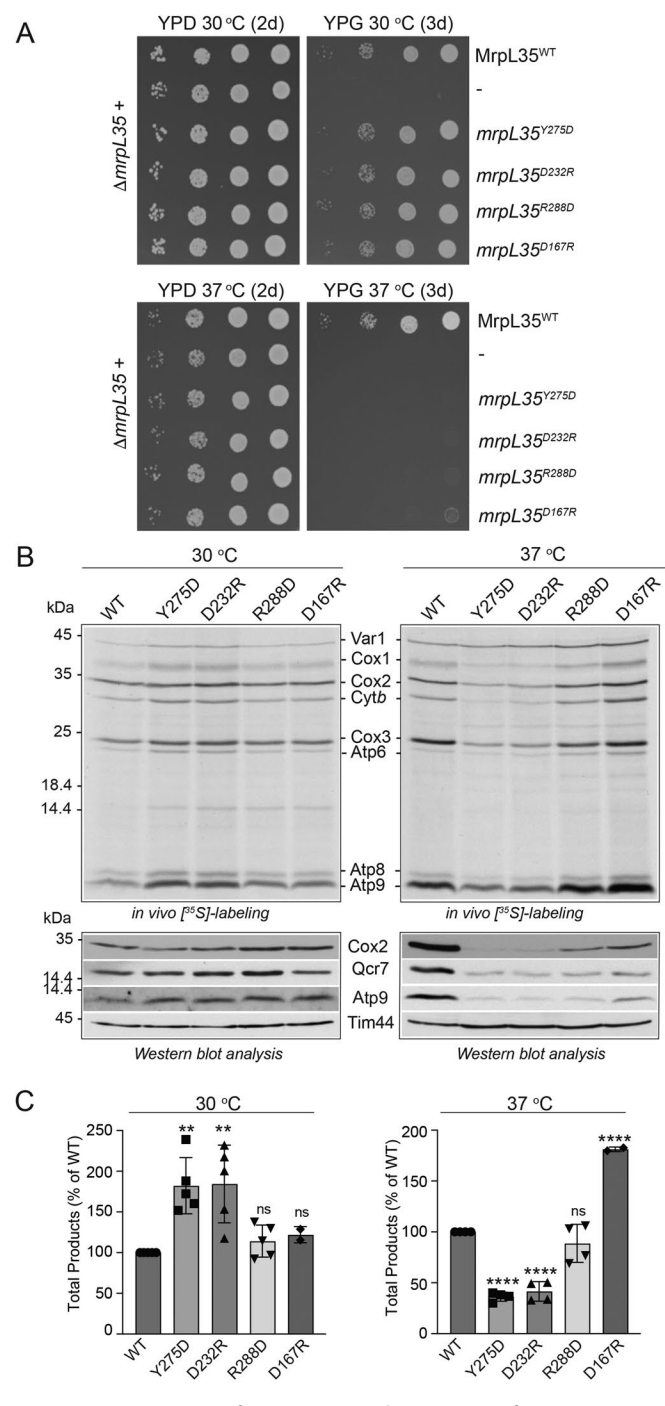


FIGURE 3: Mutation of Asp(D)232 and Arg(R)288 of MrpL35/mL38 causes a disconnect between mitochondrial translation and OXPHOS assembly. A) Growth phenotype analysis on glucose (YPD; 2d) or glycerol (YPG; 3d) of indicated strains was performed as described in Figure 2A. B) In vivo labeling of mitochondrial translation with [35S]methionine, followed by extraction of total cellular proteins, SDS-PAGE analysis, Western blotting, autoradiography. Subsequent immunedecorations with indicated mrpL35 strains, was performed as described in Figure 2B. The immunedecoration data from multiple independent Western blots were quantified and summarized in Supplemental Figure S2B. C) The sum of total radiolabeled products synthesized in each strain analyzed in B) was quantified, as described in Figure 2C. Data from independent experiments and autoradiographs (n = 2-5) are provided. Comparison of each mrpL35 mutant to its respective WTmcontrol, resulted in either no significant difference (ns), or

including in the *mrpL35*R288D mutant where the mitochondrial translation activity was not compromised and paralleled that of the WT control (Figure 3B, lower right panel; Supplemental Figure S2B). Furthermore, the reduction in OXPHOS content in the *mrpL35*D232R and *mrpL35*R288D mutants grown at 37°C was more pronounced than observed in the *mrpL35*D232A and *mrpL35*R288A mutants at this temperature (Figure 2B; Supplemental Figure S2, A and B). We conclude that the introduction of a residue of opposite charge in these positions of MrpL35/mL38 was more detrimental to function than having no charge. Together with the Ala(A) mutation results, these data indicate that the mutation of residues Asp(D)232 and Arg(R)288 impairs the ability of MrpL35/mL38 to support OXPHOS assembly in particular at elevated stress temperatures, and the primary cause of this defect does not appear to be attributed to a parallel inhibition of the mitotranslation process per se.

Residues Asp(D)232 and Arg(R)288 may function together to ensure MrpL35/mL38's ability to support effective OXPHOS complex assembly

PEBP-invariant residues Asp(D)232 and Arg(R)288 of MrpL35/mL38 are located in two highly conserved aspects of PEBP proteins known as the DPDxP and GxHR motifs of the CR1 and CR2 regions, respectively, and which together form critical aspects of the putative ligand binding pockets of the PEBP domains (Figure 1A). Structural analysis of mammalian and plant PEBP proteins, have shown that the PEBP-invariant residues corresponding to MrpL35/mL38's Asp(D)232 and Arg(R)288 residues, that is, bovine Asp(D)71 and Arg(R)118, interact through a salt-bridge arrangement (Banfield et al., 1998; Serre et al., 1998, 2001; Banfield and Brady, 2000; Mima et al., 2005; Gombault et al., 2007). The available cryoEM structures of yeast mitoribosomes (Amunts et al., 2014; Desai et al., 2017) support that Asp(D)232 and Arg(R)288 residues of MrpL35/ mL38 are also sufficiently close to each other to be paired in a saltbridge formation (predicted 2.8-3.3 as Å's distance; Figure 4A) and thus the elimination of a charge by an Ala(A) substitution, or the exchange for a residue of opposite charge could adversely impact their potential salt-bridge pairing. Whether solely present in a paired interaction, we argued that reversing both charges, that is, the creation of the double mutant mrpL35D232R;R288D may result in a functional mrpL35 protein. Respiratory-based growth mrpL35D232R;R288D mutant (Figure 4B) however resembled that of the mrpL35D232A;R288A mutant (Figure 2B) by exhibiting a strong growth defect at 37°C, indicating that the double charge reverse mutant did not fully restore MrpL35/mL38's function. After an extended incubation period on glycerol at 37°C, we routinely observed the emergence of a small number of single-cell colony, suppressor-like strains in the mrpL35D232R;R288D samples, which were notably absent in the mrpL35D232A,R288A samples (unpublished results). When a representative suppressor strain was isolated and cultivated, its growth was barely apparent at 37°C, and remained strongly reduced in comparison to the WT MrpL35/mL38 control (Figure 4B). Although not genetically further analyzed here, the emergence of the suppressors in the mrpL35D232R;R288D mutant is indicative that the double charge reverse may have conferred a slight functional advantage to MrpL35/mL38 over the double Ala(A) mutant. Finally, the lack of ability of the $mrpL35^{D232R;R288D}$ to fully restore growth to the $\Delta mrpL35$

in a significant difference and as indicated by **, p < 0.01; ****, p < 0.0001. Strains: WT MrpL35/mL38; Y275D, mrpL35^{Y275D}, D232R; mrpL35^{D232R}; R288D, mrpL35^{R288D}; D167R, and mrpL35^{D167R}.

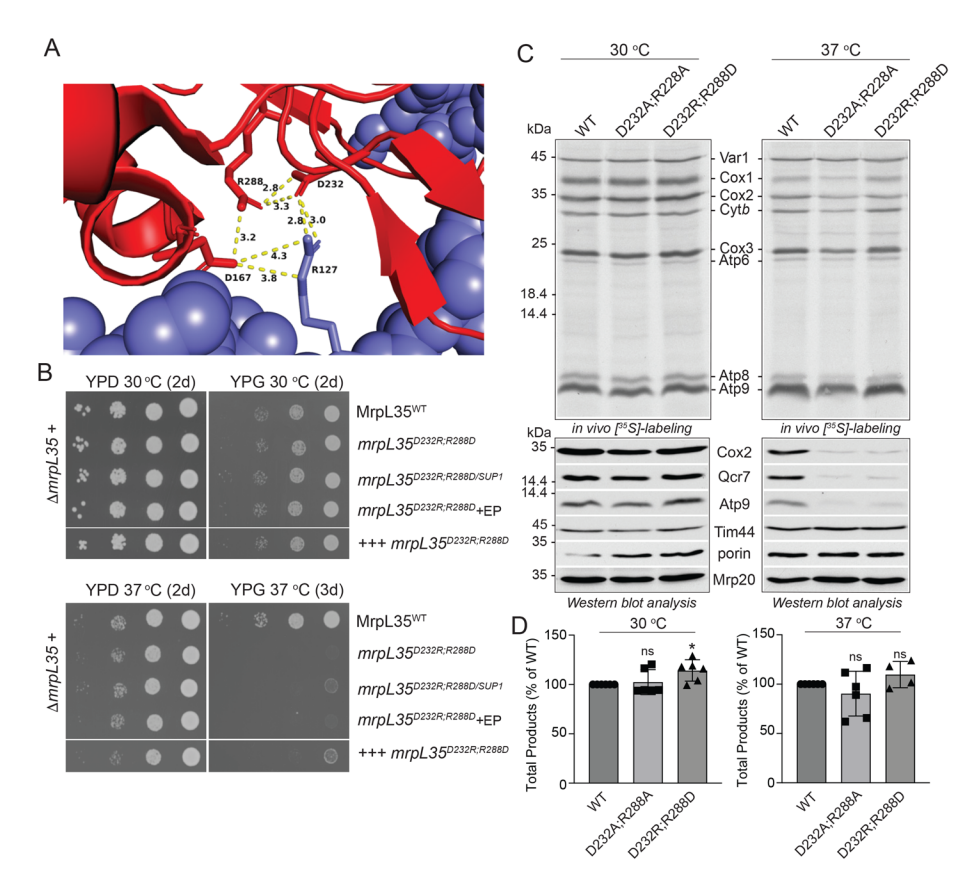


FIGURE 4: Residues Asp(D)232 and Arg(R)288 of MrpL35/mL38 exist in close proximity to each other and together are required for ensuring effective assembly and stability of newly synthesized proteins. A) PyMol image of S. cerevisiae MrpL35/mL38 (red) protein (from PDB 5MRC), illustrating proximity of residues (approximate Å distances indicated) Asp(D)232 and Arg(R)288 to each other and also to Arg(R)127 of Mrp7/bL27m (slate blue) and Asp(D)167 of MrpL35/mL38, respectively. B) Growth phenotype analysis of indicated strains was performed as described in Figure 2A and incubated for number of days indicated. Note independent suppressor strains are visible in the mrpL35D232R;R288D samples after 6 d growth on YPG at 37°C (unpublished data). One such independent suppressor isolated from the mrpL35^{D232R;R288D} strain after prolonged growth at 37°C was also analyzed in parallel, as indicated by mrpL35D232R;R288D/SUP1. The mrpL35D232R;R288D strain harboring the pVT100U-ADHmrpL35^{D232R;R288D} plasmid (indicated by +++ mrpL35^{D232R;R288D}) to constitutively overexpress the mrpL35D232R;R288D protein was also analyzed together with its control, the mrpL35D232R;R288D strain transformed with the empty (i.e., not insert) pVT100U-ADH1 plasmid (EP), as indicated by $\mathit{mrpL35^{D232R;R288D}}+EP.$ C and D) In vivo radiolabeling of mitotranslation was monitored in indicated mrpL35 strains grown in galactose-media at 30°C (left panels) or 37°C (right panels), as described in Figure 2B. Cell extracts were analyzed by SDS-PAGE, Western blotting, and autoradiography (C, upper panels). Immunedecorations were also performed (C, lower panels) to analyze steady-state levels of indicated OXPHOS subunits and the Mrp20/uL23m (Mrp20) protein; Tim44 and porin were used as loading controls. The OXPHOS subunit immunedecoration data from multiple independent Western blots were quantified and summarized in Supplemental Figure S2C. D) The sum of total radiolabeled products synthesized during the in vivo radiolabeling assay in B) was determined, as described in Figure 2C. The analysis of two independent autoradiographs of technical replicates each from two or three independent experiments, as indicated, was performed. The significance between measurements was determined by one-way ANOVA using GraphPad Prism 9. Comparison of each mrpL35 mutant to its respective WT control, resulted in either no significant difference (ns) or in a significant difference (*, p < 0.1), as indicated. Strains: WT MrpL35/mL38; D232A;R288A, mrpL35^{D232A;R288A}; D232R;R288D, and mrpL35^{D232R;R288D}.

strain was not due to an indirect effect of potentially limiting levels of the mutant mrpL35 protein because when overexpressed from a high copy-number plasmid and under control of strong, constitutive ADH1 promoter, the mrpL35^{D232R;R288D} protein did not rescue the growth of the $\Delta mrpL35$ mutant (Figure 4B).

vivo radiolabeling analysis galactose-grown cells indicated that the mrpL35^{D232R;R288D} mutant. like mrpL35^{D232A;R288A} mutant, exhibited normal levels of mitochondrial translation when cultivated at 30 and 37°C, including normal levels of Var1 synthesis (Figure 4, C and D). Consistently, analysis of the mitochondrial ribosome content of these mutants (as measured by levels of Mrp20/uL23) demonstrated that levels were not reduced relative the WT control (Figure 4C, lower panels) and even determined to be slightly elevated (Mrp20/uL23m levels in both mutants at 37°C were determined to be ~120% of WT control). Whereas a slight reduction in translational output was observed in the mrpL35^{D232A;R288A} mutant at the nonpermissive temperature of 37°C, mitotranslation in the $mrpL35^{\rm D232R;R288D}$ mutant closely resembled the WT MrpL35/ mL38 control (Figure 4, C, upper right panel and D). Despite the robust mitochondrial protein synthesis output of these mutants, a strong decrease in OXPHOS complex levels, as indicated by Cox2, Qcr7, and Atp9 steady-state levels, was observed in the mrpL35^{D232R;R288D} mutant when cultivated on galactose at 37°C, where they appeared similar to those in the $mrpL35^{D232A;R288A}$ mutant (Figure 4C, right lower panels; Supplemental Figure S2C). When analyzed at the permissive temperature of 30°C, mitochondrial protein synthesis output in both mutants was similar, or even slightly elevated, from the WT control. Cellular OXPHOS levels appeared normal also in these mutants when grown at the permissive temperature. A similar result was also obtained when the mrpL35D232A;R288A mutant was grown in glycerol (respiratory) medium at the permissive temperature, illustrating the balance of protein synthesis and OXPHOS assembly was similar in this mutant under both fermentation (galactose) and respiratory growth conditions (Supplemental Figure S4).

In summary, as MrpL35/mL38 is essential for normal mitoribosomal assembly and for protein translation (Zeng et al., 2018), we can conclude from the retention of the translational capacity in the mrpL35 mutants that the introduced mutations did not render MrpL35/mL38 (or Var1) potentially instable and thus limiting in levels for ribosomal translation per se. Rather, we conclude that when performed under elevated

temperatures, in contrast to permissive temperatures, the process of mitochondrial protein synthesis in the mrpL35D232A;R288A and mrpL35^{D232R;R288D} mutants yields proteins with impaired competency and/or availability to be effectively assembled into OXPHOS complexes.

Residues Asp(D)232 and Arg(R)288 of MrpL35 are in close vicinity of Asp(D)167 of MrpL35/mL38 and Arg(R)127 of Mrp7/bL27m

The inability of the double charge reversal mutant mrpL35D232R;R288D to fully restore the function of MrpL35/mL38 to ensure mitotranslation yielded assembly competent nascent chains could indicate that Asp(D)232 and Arg(R)288 may not be exclusively present in a saltbridge paired relationship with each other, but that these residues may (also) interact with other charged residues in their proximity. Residues Asp(D)232 and Arg(R)288 of MrpL35/mL38 are located in a "charged" microenvironment, which includes Asp(D)167 of MrpL35/mL38 and Arg(R)127 in the C-terminal mitospecific domain of the neighboring Mrp7/bL27m protein (Figure 4A) The measured distance of 2.8-3.0 Å between Asp(D)232 of MrpL35/mL38 and Arg(R)127 of Mrp7/bL27m could also indicate a possible functional pairing between these residues. Likewise, the closeness of Arg(R)288 and Asp(D)167 residues (3.2 Å measured distance) of MrpL35/mL38 could suggest that these residues may directly interact and support each other too.

To further investigate the possible functional significance of this charged residue arrangement, we created mutant yeast strains harboring either Asp(D)167 mutated derivatives of MrpL35/mL38 or Arg(R)127 mutants of Mrp7/bL27m. We individually mutated these residues either to neutral Ala(A) (i.e., mrpL35^{D167A} or mrp7^{R127A}) or to residues of opposite charge (i.e., mrpL35^{D167R} or mrp7^{R127D}), as given the charge cluster arrangement of these residues, we anticipated the introduction of opposite charges may be more detrimental than introduction of a neutral Ala(A) substitution, as we had observed with the Asp(D)232 and Arg(R)288 mutants.

Expression of the mrpL35D167A derivative restored the respiratory-based growth defect of the $\Delta mrpL35$ null mutant strain at both 30 and 37°C, as growth of the mrpL35D167A strain mirrored that of the WT MrpL35/mL38 control (Figure 2A). While the mrpL35^{D167R} mutant appeared to grow normally at 30°C, a strong growth defect was observed at the stress temperature of 37°C on glycerol, the nonfermentable carbon source, illustrating the deleterious impact of the introduction of a positive charge into this region of MrpL35/ mL38 (Figure 3A). Mitochondrial translation, as monitored by in vivo radiolabeling with [35S]methionine, was not compromised in the $mrpL35^{\mathrm{D167A}}$ and $mrpL35^{\mathrm{D167R}}$ mutants grown when both at 30 and 37°C (Figures 2, B and C; 3, B and C), indicating that removal or reversal of the charged residues at this position did not inhibit MrpL35/ mL38's ability to support mitochondrial translation. Despite an observed elevation in level of mitochondrial protein synthesis in the mrpL35^{D167R} mutant when grown at 37°C, a strong decrease in cellular OXPHOS enzyme content (as indicated by Cox2, Qcr7, and Atp9 levels) was observed, consistent with the impaired respiratory growth behavior of this mutant observed at the stress temperature (Figure 3B, right lower panel; Supplemental Figure S2B). On the other hand, cellular OXPHOS content levels were only slightly reduced in the mrpL35^{D167A} mutant at 37°C (Figure 2B; Supplemental Figure S2A), consistent with the observed ability of this mutant to support normal respiratory-based growth at the elevated temperature (Figure 2A).

Independent mutational analysis of residue Arg(R)127 of the neighboring Mrp7/bL27m protein, highlighted the importance of this charged residue also (Figure 5). The presence of Mrp7/bL27m is required for respiratory-based growth and mutation of residue Arg(R)127 of Mrp7/bL27m to a neutral Ala(A) residue, that is, mrp7^{R127A} did not appear to impact Mrp7/bL27m's ability to support growth on the nonfermentable carbon source glycerol at 30 or 37°C (Figure 5A). On the other hand, exchange of this residue with one of

an opposite charge, that is, *mrp7*R127D, proved more deleterious for Mrp7/bL27m's ability to support growth, as impaired growth capacity was observed on glycerol medium at 37°C. The importance of the presence of a charged residue in this position of Mrp7/bL27m was indicated by the observation that substitution of Arg(R)127 with another positively charged residue, Lys(K), that is, the *mrp7*R127K, did not negatively impact Mrp7/bL27m's ability to support respiratory-based growth of the result mutant (Figure 5A).

In vivo radiolabeling experiments with [35S]methionine indicated that the mitoribosome translational capacity appeared not to be adversely affected through the *mrp*^{7R127A} or *mrp*^{7R127D} mutations, at 30 or 37°C (Figure 5, B, upper panels and C). However, consistent with the reduced growth at the elevated temperature, a reduction in the steady state levels of OXPHOS complex subunits Cox2, Qcr7, and Atp9 was measured in the *mrp*^{7R127D} mutant grown at 37°C (Figure 5B, right lower panel; Supplemental Figure S2D). We therefore conclude that charged nature of the residue Arg(R)127 of Mrp7/bL27m and location in close proximity to the Asp(D)167, Asp(D)232, Arg(R)288 of MrpL35/mL38, is important for Mrp7/bL27m's ability to support the assembly of the OXPHOS system in yeast mitochondria.

The impaired OXPHOS capacity of the mrpL35 mutants is not due to a compromised Pth4 protein

In the human mitoribosome a close structural relationship has been shown to exist between mL38 and an externally facing protein termed MRPL58/ICT1. ICT1 is a putative peptidyl-tRNA hydrolase, which may function to release the polypeptide from the peptidyl tRNA from ribosomes stalled during the translational process (Richter et al., 2010; Akabane et al., 2014; Chicherin et al., 2021; Kummer et al., 2021). Although the yeast homologue of ICT1, Pth4, has not been found as a structural component of the yeast mitoribosome (Dujeancourt et al., 2013; Amunts et al., 2014; Hoshino et al., 2021), we cannot exclude the possibility that a transient relationship between MrpL35/mL38 and Pth4 may exist. We therefore probed whether the OXPHOS assembly defects observed in the mrpL35 mutants simply reflected a compromised Pth4 protein function. The PTH4 gene was genetically knocked out in the WT MrpL35/mL38 and mrpL35D232R, mrpL35Y275D, and mrpL35R288D mutant cells and the impact of the absence of Pth4 on cellular levels of mitochondrial translation and OXPHOS complex assembly was then analyzed in cells grown at 30 and 37°C (Figure 6, A and B). In WT MrpL35/mL38 cells, absence of Pth4 protein was correlated with a minor reduction in overall mitochondrial translational levels at 37°C (Figure 6B). Western blotting of Cox2, a representative OXPHOS subunit, indicated that the absence of Pth4 did not significantly compromise the levels of the COX complex in WT MrpL35/mL38 cells when grown at 30 or 37°C (Figure 6, A and B, lower panels). We conclude that Pth4 is not required for mitochondrial translation or the subsequent assembly of nascent chains into stable OXPHOS enzymes, consistent with previous reports (Hoshino et al., 2021). The absence of Pth4 in the mrpL35 mutants analyzed had a similar effect as in WT cells, that is, did not greatly impact the overall mitoribosomal translation activity levels at 30 or 37°C and resulted in a minor decrease (in the already strongly decreased levels) of OXPHOS complexes in each of the mrpL35 mutants grown at 37°C. Comparing the phenotypes of the WT MrpL35;∆pth4 cells (i.e., continued mitotranslation and a minor impact on OXPHOS complex levels) versus those of the mrpL35 mutants ± Pth4 (i.e., the continued mitotranslation, but strongly compromised OXPHOS assembly levels), the phenotypes of the mrpL35 mutations were significantly more deleterious than those caused by the absence of Pth4 alone. We therefore conclude

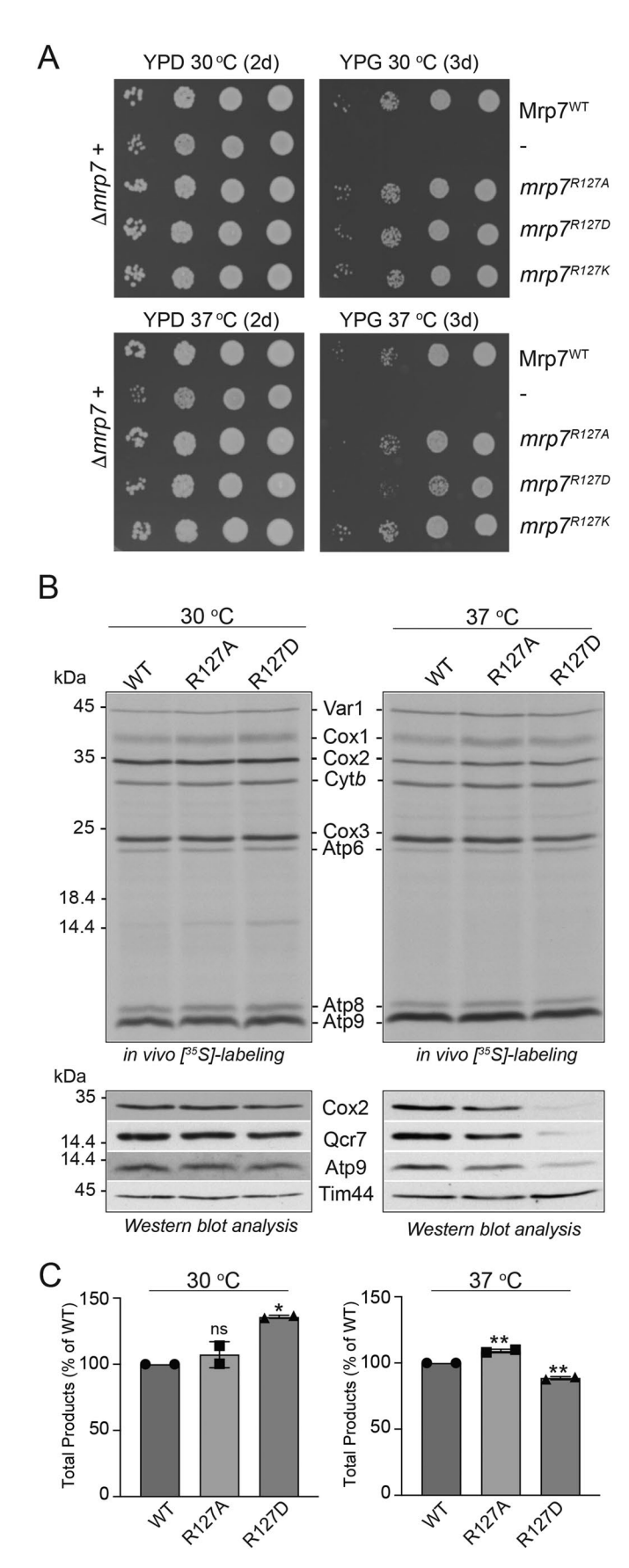


FIGURE 5: Residues Arg(R)127 of Mrp7/bL27m is important to ensure mitotranslation yields products competent for OXPHOS assembly. A) 10-fold serial dilutions of $\Delta mrp7$ strains with pRS413

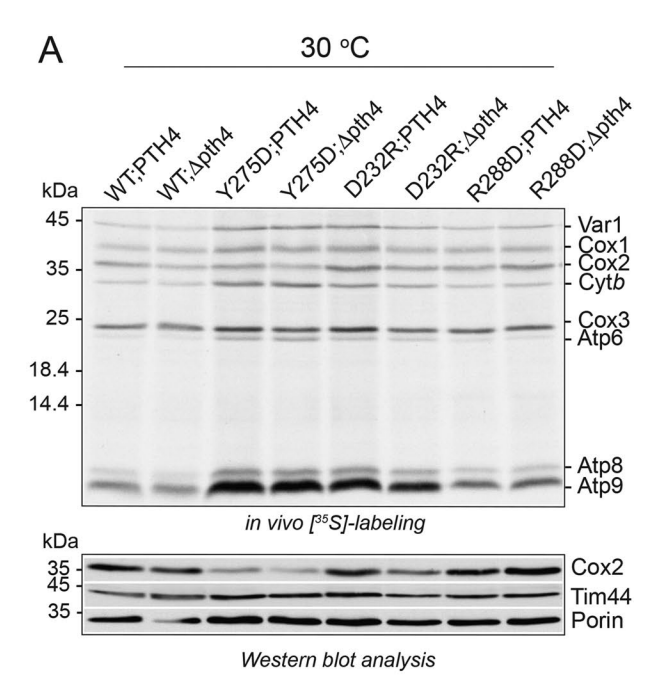
the OXPHOS assembly defects observed in the mrpL35 mutants cannot be simply attributed to an impaired Pth4 function, but rather reflect the compromised ability of the mitoribosome to synthesize proteins with the ability and/or opportunity to assemble into stable OXPHOS complexes.

DISCUSSION

The mL38 proteins are mitochondrial-specific ribosomal proteins found through diverse eukaryotic cells. Forming key components of the CP region of the mitoribosome, mL38 proteins from diverse species are unified by the presence of their PEBP-homology domain. The polar nature of the "nearly invariant" PEBP residues has led to the speculation that the ligand binding cavities of PEBP proteins may represent catalytically active centers, rather than inert ligandbinding sites, and that the PEBP proteins, involved in diverse signaling pathways, may have enzymatic functions related to small molecule (e.g., sugars or ribonucleoside moieties) metabolism (Tsoy and Mushegian, 2022). Although the available cryoEM mitoribosomal structures indicate that mL38 proteins are structurally similar to PEBP proteins with their characteristic ligand binding cavities, the mL38 proteins form a separate evolutionarily diverged clade of the PEBP family, as several of the "nearly invariant" polar PEBP residues characteristic of the "classical PEBP members" are not universally preserved among the mL38 family members (Tsoy and Mushegian, 2022). This sequence divergence has led to the speculation that the mL38 clade of PEBP proteins may have acquired a new molecular function through evolution (Tsoy and Mushegian, 2022). Given the structural conservation of PEBP ligand binding cavity of mL38, and its external exposure on the surface of the CP, a key regulatory region of the mitoribosome, it is tempting to speculate that while the mL38 proteins may not represent catalytically active PEBP members, they may have retained the capacity to bind and respond to a small molecule ligand or regulator through their PEBP-like domains, possibly to modulate an aspect of the mitoribosomal translational process.

To support that features of the PEBP ligand binding cavity are important to MrpL35/mL38's function, our results here demonstrate that the two PEBP "nearly invariant" polar residues conserved among mL38 family members, and equivalent to Asp(D)232 and Arg(R)288 of yeast MrpL35/mL38, are critical for the ability of MrpL35/mL38 to support respiratory-based growth of the cell,

plasmid containing no insert (-), or a gene insert encoding the WT Mrp7/bL27m protein (Mrp7^{WT}) or a mutated *mrp7* derivatives, as indicated. Cells were plated and grown as described in Figure 2A. B and C) In vivo radiolabeling of mitotranslation was monitored in indicated mrp7 strains grown in galactose medium at 30 or 37°C, as described in Figure 2B. Cell extracts were analyzed by SDS-PAGE, Western blotting, and autoradiography (B, upper panels), followed by phosphorimaging C), as described in Figure 3C. Immunedecorations were also performed (B, lower panels) to analyze the steady state levels of indicated OXPHOS subunits in each strain; Tim44 was used as a loading control. The OXPHOS subunit immunedecoration data from independent Western blots were quantified and summarized in Supplemental Figure S2D. C) Phosphorimager analysis of two independent autoradiographs of technical replicates was performed. The significance between measurements was determined by one-way ANOVA using GraphPad Prism 9. Comparison of each mrp7 mutant to its respective WT control, resulted in either no significant difference (ns), or in a significant difference and as indicated by *, p < 0.05; **, p < 0.01. Strains: WT Mrp7/bL27m; R127A, $mrp7^{R127A}$; R127D, and mrp7^{R127D}.



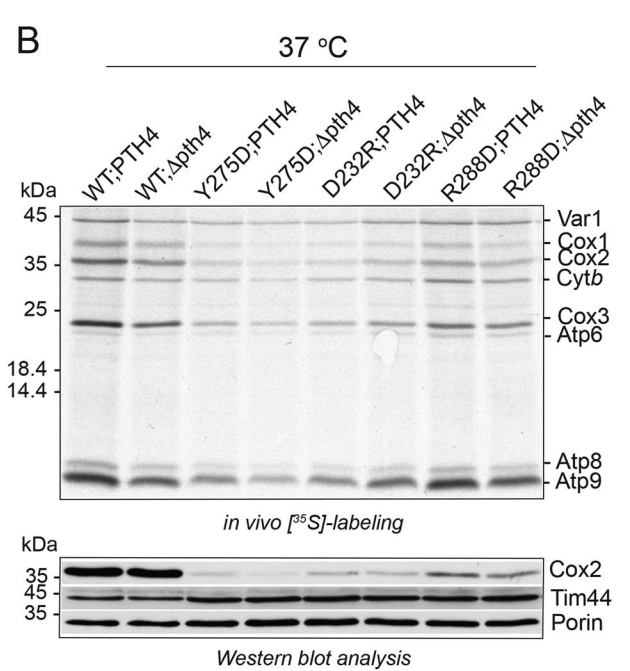


FIGURE 6: OXPHOS assembly defects observed in the *mrpL35* mutants are not due to the functional absence of Pth4, the yeast ICT1 homolog. A and B) The indicated strains were propagated in galactose medium at 30°C A) or 37°C B) and in vivo radiolabeling of mitotranslation was monitored in the presence of [³⁵S]methionine and as described in Figure 2B. Cell extracts were analyzed by SDS–PAGE, Western blotting, and autoradiography (upper panel) and through immunedecorations (lower panels) to analyze the steady-state levels of indicated OXPHOS subunits; Tim44 and porin were used as loading controls. Strains: PTH4 or Δ*pth4* indicates the presence or absence of the PTH4 gene, respectively in the following yeast strains: WT MrpL35/mL38; Y275D, *mrpL35*Y275D; D232R, *mrpL35*D232R, R288D, and *mrpL35*R288D.

especially under temperature-stress conditions. Mutation of the Asp(D)232 and Arg(R)288 residues had significant impact for MrpL35/mL38's ability to ensure normal steady state levels of

OXPHOS complexes cytochrome bc_1 , COX and F_1F_0 -ATP synthase at elevated growth temperatures (37°C). The corresponding invariant residues in other PEBP proteins (e.g., bovine PEBP1 Asp[D]71 and Arg[R]118) have been shown to be physically associated with each other through a salt-bridge arrangement (Banfield et al., 1998; Serre et al., 1998, 2001; Banfield and Brady, 2000). While the phenotypic impact of the individual mutation of either Asp(D)232 or Arg(R)288 would support a similar arrangement of these residues in yeast MrpL35/mL38 protein, it is important to note that our findings may suggest that Asp(D)232 and Arg(R)288 may not be exclusively present in a salt-bridge formation. Mutation of Asp(D)232 (to an opposite charge) appeared more deleterious in terms of supporting mitochondrial translation than the corresponding chargereverse mutation of Arg(R)288. Second, the double Ala(A) mutant, mrpL35^{D232A;R288A} performed significantly worse at supporting respiratory-based growth than either of the individual single Ala(A) mutants, and finally, the double charge reverse mutant, mrpL35^{D232R;R288D}, did not restore function, even when overexpressed. The mrpL35D232R;R288D mutant, unlike the mrpL35D232A;R288A mutant, also yielded some spontaneous suppressor strains, which exhibited a partial restoration of respiratory growth at elevated growth temperatures. While Asp(D)232 and Arg(R)288 may exist in a relationship with each other, based on our findings, we consider it possible when one or other is mutated, or during a natural dynamic conformational change of the MrpL35/mL38 protein, that other charged residues in their vicinity may also play a supportive (and dynamic) role. Our data presented here would support that residues Asp(D)167 of MrpL35/mL38 and Arg(R)127 of Mrp7/ bL27m are important for the function of their respective proteins and may represent alternative partners to Asp(D)232 and Arg(R)288 of MrpL35/mL38, respectively.

It is important to note that while our data highlight the importance of the PEBP invariant residues Asp(D)232 and Arg(R)288 residues for the function of mitoribosomal MrpL35/mL38 protein to support the respiratory activity of the cells, our in vivo labeling analysis would indicate that the primary cause of the OXPHOS deficiency observed in the mrpL35 mutants cannot be attributed to a corresponding inhibition in the mitochondrial translational process per se. A severe respiratory growth defect and a decrease in steady state levels of OXPHOS complexes were recorded in the mrpL35D232A;R288A and mrpL35D232R;R288D mutants (as well as in the corresponding single Asp(D)232 and Arg(R)288 mutants) when grown at 37°C, yet the levels mitochondrial protein translation remained largely unaffected in these cells. A similar disconnect between the process of mitochondrial protein synthesis and the opportunity and/or competency of newly synthesized proteins to assemble into OXPHOS complexes, was also observed in the mrpL35^{D167R} and mrp7^{R127D} mutants at the nonpermissive temperature. From the observed retention of mitochondrial translational capacity in the analyzed mrpL35 and mrp7 mutants, we can infer that the assembly and stability of the mitoribosome, and thus MrpL35/ mL38's interactions with other mitoribosomal proteins and/or its own functional levels (or the content of mitoribosomal subunit Var1) were not grossly perturbed through these mutations. We therefore conclude that the deleterious impact of these mutations was independent of the mitoribosomes ability to perform translational process per se but rather resulted in a change which adversely affected the posttranslational fate of the resulting newly synthesized proteins.

Why do these CP mutations, which have little effect on mitochondrial translation in terms of translational output levels, result in newly synthesized proteins perturbed in their assembly into

OXPHOS complexes? Assembly of mtDNA encoded proteins to form stable and functioning OXPHOS enzymes is a multistep process. It requires not only the synthesis of mtDNA encoded proteins, but also their folding, membrane insertion (with correct topology attainment), prosthetic group/cofactor incorporation and stepwise unification with their nuclear encoded OXPHOS partners. The fidelity, rate (including possible need for pausing of translation to ensure cotranslational membrane insertion), and the location of translation (with respect to both membrane insertion sites and the meeting zone for assembly with imported nuclear encoded partners) are all critical steps in the OXPHOS complex assembly process. A failure of the mitoribosome to effectively perform one or more of these critical steps, may not result in a protein synthesis defect per se, but could potentially contribute to the compromised opportunity and/ or competency for the newly synthesized protein to effectively assemble to form an OXPHOS complex. No accumulation of the precursor species of Cox2 (pCox2) was observed in any of the mrpL37 or mrp7 mutants analyzed in this study. The pCox2 species is processed to its mature form by the Imp1 peptidase on the intermembrane space side of the inner membrane (Hell et al., 1997). The absence of a pCox2 species is an indication that at least the initial cotranslational insertion of the N-terminal region of this protein has successfully proceeded in these mutants. It is important also to consider that the reduction in OXPHOS complex content observed in the mrpL35 mutants despite ongoing mitotranslation, could in theory be attributed to compromised expression of the nuclear encoded OXPHOS partner subunits in these mutants. Hypothetically, this scenario could occur if MrpL35/mL38 and/or the CP region of the mitoribosome were to be involved in a signaling pathway to the nucleus to influence the expression of nuclear genes that encode mitochondrial proteins and normally repressed under non-OXPHOS promoting conditions (e.g., glucose fermentation). Failure to engage this hypothetical signaling mechanism in the mrpL35 mutants would result in continued mitoprotein synthesis (nuclear encoded mitoribosome and import machinery components are not encoded by glucose-repressed genes [Morgenstern et al., 2017]) but uncoupled from downstream OXPHOS assembly events due to the limiting levels of available nuclear encoded OXPHOS protein partners. While we cannot rule out the possibility from our current analysis, we noted the levels of another glucose repressed (non-OXPHOS) nuclear encoded protein porin was unaffected in the mrpL35 mutants analyzed (e.g., Figures 4C and 6) suggesting that the regulated expression of nuclear encoded mitochondrial proteins may not be globally compromised in these mrpL35 mutants. Rather, to explain the observed reduction in OXPHOS content in the mrpL35 mutants we favor a model where the disconnect between the processes of mitotranslation and the OXPHOS assembly as a result of the mutations of MrpL35/mL38 and Mrp7/bL27m reported here may be one caused by impact to the fidelity, timing, and/or location of the translational process. The CP region of the mitoribosome has the potential to influence the translational process and its fidelity, as CP proteins MrpL28/mL40 and Mrp7/bL27m extend via their N-termini directly into the PTC of the ribosome, where in the human mitoribosome they have been shown to interact with the tRNAs at the Aand/or P-site, respectively (Amunts et al., 2014, 2015; Brown et al., 2014, 2017; Aibara et al., 2020). The MrpL35/mL38 protein forms close partnership with the C-terminal domains of both MrpL28/ mL40 and Mrp7/bL27m within the CP, making it possible that conformational changes in mL38 for example, upon ligand binding at its PEBP domain, could be communicated to exert an influence on the PTC of mitoribosome, via the partner mL40 and bL27m proteins. We observed that the newly synthesized Cox1 and Cox2 proteins were more susceptible to enhanced proteolytic turnover in the $\it mrpL35^{D232A;R288A}$ mutant (unpublished results), which would be consistent with a translational fidelity or folding defect and may be a contributing factor to the observed particular susceptibility of the COX assembly process in the mutants. However, increased proteolytic turnover of newly synthesized proteins was not the case for the other mitoribosomal synthesized proteins (Var1, Cytb, Cox3, and Atp6; unpublished results). The latter class of newly synthesized proteins displayed similar proteolytic turnover patterns in the mrpL35^{D232A,R288A} in pulse chase experiments as their counterparts in WT control, making it unclear whether alterations in the fidelity of translation is the primary underlying defect in the mrpL35 mutant.

In addition to actually synthesizing the mtDNA encoded proteins, we propose here that the mitoribosome may have a part in determining the posttranslational fate of its synthesis products. We have recently speculated that the mitoribosome is primed to function differently under respiratory metabolic conditions when OXPHOS assembly is promoted versus glucose-fermentation conditions where proteolytic turnover of the mitotranslation products is in contrast prioritized (Anderson et al., 2022). Our findings here indicate that the CP region, specifically MrpL35/mL38 and its PEBP ligand binding domain, may play a key role to ensure this differential "priming", possibly by binding a metabolic ligand specifically which is enriched in the mitochondrial matrix under respiratory promoting conditions. The limited availability of this ligand under glucose fermentation conditions (or a limited binding capacity when the integrity of the mL38 ligand binding pocket may be perturbed through mutation) would favor a mitoribosome primed to promote translation but physically uncoupled from downstream OXPHOS assembly events. The mrpL35 PEBP mutants analyzed here may thus function to prime the mitoribosome under stress temperatures to operate independently from the downstream assembly events, normally designed to optimize OXPHOS complex assembly under respiratory demanding growth conditions (Dennerlein and Rehling, 2015; Dennerlein et al., 2017; Anderson et al., 2022).

In sum, due to the genetically mosaic nature of the mitochondrial OXPHOS complexes, the mitochondrial ribosome, in contrast to its bacterial ancestor, needs to have evolved regulatory mechanisms to ensure its translational activity is coordinated with nuclear gene expression when needed to respond to cellular needs promoting OXPHOS complex assembly. We speculate here that mitospecific ribosomal proteins such as mL38 may serve to differentially prime and regulate the mitoribosome, and in doing so, contribute to the posttranslational fate of the newly synthesized proteins. Future experiments will address the nature of the putative ligand binding to the PEBP homology domain of the mL38 proteins.

MATERIALS AND METHODS

Yeast strains and growth conditions

All strains used in this study are derivatives of the S. cerevisiae haploid W303-1A genetic background (W303-1A, mat a, leu2, trp1, his3, and ade2). They include the ∆mrpL35 (MRPL35::KAN) and Δmrp7 (MRP7::KAN) mutant strains, with a pRS413 plasmid borne WT MRPL35/mL38 or MRP7/bL27m (Box et al., 2017; Anderson et al., 2022) or mutant gene derivatives, as indicated. The chromosomal PTH4 open reading frame was replaced through homologous recombination in the WT MrpL35/mL38 and indicated mrpL35 mutant yeast strains using a PCR-amplified URA3 cassette flanked by 5' and 3' PTH4 gene specific sequences and confirmed through analytical PCR. All strains were cultured using standard protocols on minimal synthetic medium (S)

supplemented with (when appropriate) uracil, tryptophan, leucine, adenine, or whether indicated, on full YP (Yeast extract, peptone) media, with glucose (2%), galactose (2%), or glycerol (3%) as carbon source, as indicated.

Generation of mrpL35 and mrp7 mutants

PCR-based site directed mutagenesis was performed to create the indicated mrpL35 mutants using the previously cloned pRS413based plasmid containing WT MRPL35/mL38 open reading frame and 5' and 3' regulatory regions (Box et al., 2017) as the template DNA. Mutation of targeted codon(s) was verified following sequencing of the entire mrpL35 gene insert and the resulting recombinant pRS413 plasmid was introduced into the haploid $\Delta mrpL35$ yeast strain harboring the WT MRPL35 gene on a pRS316 (URA3) plasmid (Box et al., 2017). A plasmid shuffling approach using 5-fluoroorotic acid (5'FOA) was used to exchange the pRS316-based plasmid for the pRS413-mrpL35 mutant plasmid, or when indicated, for a pRS413 plasmid harboring the control WT MRPL35 gene fragment or no insert, that is the pRS413 "empty" plasmid (i.e., no insert), and as previously described (Box et al., 2017). A similar approach was adopted to create the mrp7 Arg(R)127 mutant yeast strains and using the $\Delta mrp7$ haploid yeast strain and pRS316 and pRS413-based MRP7 and mrp7 mutant gene inserts, as previously described (Anderson et al., 2022). The use of a centromeric plasmid (pRS413) and employment of the endogenous MRPL35 (or MRP7) 5' and 3' regulatory regions to drive expression of MrpL35/mrpL35 (and Mrp7/mrp7 derivatives) was designed to mimic the expression of the mutated protein derivatives at levels similar to the endogenous MrpL35/mL38 and Mrp7/bL27m proteins. For overexpression of the mrpL35D232R;R288D derivative, the mrpL35D232R;R288D open reading frame was amplified by PCR and cloned into the pVT100U plasmid (Westermann and Neupert, 2000) engineered to contain the strong constitutive ADH1 promoter and terminator regions (pVT100U-ADH1).

In vivo radiolabeling of mitochondrial translation and extraction of cellular proteins for OXPHOS subunit steady-state analysis

Unless otherwise indicated, all yeast strains to be analyzed by in vivo radiolabeling of mitochondrial translation and/or extraction of total cellular protein for OXPHOS subunit steady-state analysis, were first passaged and cultivated on galactose-containing selective synthetic media plates, followed by growth and multiple passaging in liquid selective synthetic medium with galactose. Cells were then grown overnight (~18 h.) to mid log phase in corresponding liquid synthetic medium at 30 or 37°C, as indicated. Equivalent amounts of cells (0.6 OD₆₀₀ absorbance units) were harvested, washed, and resuspended in 40 mM phosphate buffer containing galactose, unless otherwise indicated. In vivo radiolabeling of mitotranslation with [35S]methionine was performed in presence cycloheximide (0.3 mg/ml) for 10 min at 30°C (or at 37°C when indicated), essentially as previously described (Barrientos, 2002; Barrientos et al., 2002; Anderson et al., 2022). Total cellular proteins were extracted and precipitated by TCA and analyzed by SDS-PAGE and autoradiography, and when indicated, also by Western blotting, immunedecoration (Anderson et al., 2022). Quantifications of radioactive signals from in vivo translation assays were performed by STORM phosphorimaging and subsequent analysis in ImageQuant (Cytiva Life Sciences) software. In some instances (and when indicated) ImageJ analysis of resulting autoradiographs was also performed to quantify translation levels.

Statistics and Reproducibility

All in vivo labeling experiments, Western blot/immunedecorations and serial dilution phenotype assays shown are traditionally representatives of at least three replicates. Statistical analysis was performed with GraphPad Prism 9 (Graph Pad Software) and the means and SD are provided, and when indicated, a significance analysis (one-way ANOVA) is also provided.

Miscellaneous

Multiple sequence alignments were produced with CLUSTAL O, using the default parameters. SDS-PAGE, Western blotting and immunedecorations were performed as previously described (Dienhart and Stuart, 2008). Antibodies used were against the respective purified yeast proteins and generated either in the Stuart lab or received as gifts (see *Acknowledgments*). Antigen-antibody complexes on Western blots were detected by horseradish peroxidase-coupled secondary antibodies and chemiluminescence detection on X-ray films or using the Amersham Imager 600. All images quantified by ImageJ software. BN-PAGE analysis of digitonin (1%) or DDM (0.6%) solubilized mitochondrial extracts (30 µg protein) was performed using Invitrogen Nu-PAGE gradient (3–12%) gels according to the manufacturer's protocol, followed by Western blotting and antibody decoration, as indicated.

ACKNOWLEDGMENTS

We thank Sneha Potdar, Hannah Govendik, Carmela Rios, and Yesenia Gomez for their preliminary work on the MrpL35 mutational analysis. We acknowledge and thank members of freshman BIOL 1101 (2019) lab course and Ana Paola Elias for the creation and initial analysis of the Δ*pth4* strains. We are grateful to T. Mason for the Mrp20/uL23m antibody, to V. Zara for the Qcr7 antibody, to D. Rapaport for the porin antibody and to the lab of the late Walter Neupert for the Tim44 antisera. The research was supported by National Science Foundation grant Division of Molecular and Cellular Biosciences 1817682 to R.A.S. The content is solely the responsibility of the authors and does not necessarily represent the official views of the National Science Foundation.

REFERENCES

- Aibara S, Singh V, Modelska A, Amunts A (2020). Structural basis of mitochondrial translation. Elife 9, e58362.
- Akabane S, Ueda T, Nierhaus KH, Takeuchi N (2014). Ribosome rescue and translation termination at non-standard stop codons by ICT1 in mammalian mitochondria. PLoS Genet 10, e1004616.
- Amunts A, Brown A, Bai XC, Llacer JL, Hussain T, Emsley P, Long F, Murshudov G, Scheres SHW, Ramakrishnan V (2014). Structure of the yeast mitochondrial large ribosomal subunit. Science 343, 1485–1489.
- Amunts A, Brown A, Toots J, Scheres SHW, Ramakrishnan V (2015).

 Ribosome. The structure of the human mitochondrial ribosome. Science 348, 95–98.
- Anderson JM, Box JM, Stuart RA (2022). The mitospecific domain of Mrp7 (bL27) supports mitochondrial translation during fermentation and is required for effective adaptation to respiration. Mol Biol Cell 33, ar7.
- Banfield MJ, Barker JJ, Perry AC, Brady RL (1998). Function from structure? The crystal structure of human phosphatidylethanolamine-binding protein suggests a role in membrane signal transduction. Structure 6, 1245–1254.
- Banfield MJ, Brady RL (2000). The structure of Antirrhinum centroradialis protein (CEN) suggests a role as a kinase regulator. J Mol Biol 297, 1159–1170.
- Barrientos A (2002). In vivo and in organello assessment of OXPHOS activities. Methods 26, 307–316.
- Barrientos A, Korr D, Tzagoloff A (2002). Shy1p is necessary for full expression of mitochondrial COX1 in the yeast model of Leigh's syndrome. EMBO J 21, 43–52.
- Borst P, Grivell LA (1978). The mitochondrial genome of yeast. Cell 15, 705–723.

- Box JM, Kaur J, Stuart RA (2017). MrpL35, a mitospecific component of mitoribosomes, plays a key role in cytochrome c oxidase assembly. Mol Biol Cell 28, 3489-3499.
- Brown A, Amunts A, Bai XC, Sugimoto Y, Edwards PC, Murshudov G, Scheres SHW, Ramakrishnan V (2014). Structure of the large ribosomal subunit from human mitochondria. Science 346, 718-722
- Brown A, Rathore S, Kimanius D, Aibara S, Bai XC, Rorbach J, Amunts A, Ramakrishnan V (2017). Structures of the human mitochondrial ribosome in native states of assembly. Nat Struct Mol Biol 24, 866-869.
- Chautard H, Jacquet M, Schoentgen F, Bureaud N, Benedetti H (2004). Tfs1p, a member of the PEBP family, inhibits the Ira2p but not the Ira1p Ras GTPase-activating protein in Saccharomyces cerevisiae. Eukaryot
- Chicherin IV, Dukhalin SV, Khannanov RA, Baleva MV, Levitskii SA, Patrushev MV, Sergiev PV, Kamenski P (2021). Functional diversity of mitochon drial peptidyl-tRNA hydrolase ICT1 in human cells. Front Mol Biosci 8, 716885.
- Chrzanowska-Lightowlers Z, Rorbach J, Minczuk M (2017). Human mitochondrial ribosomes can switch structural tRNAs - but when and why? RNA Biol 14, 1668-1671.
- Dennerlein S, Rehling P (2015). Human mitochondrial COX1 assembly into cytochrome c oxidase at a glance. J Cell Sci 128, 833-837.
- Dennerlein S, Wang C, Rehling P (2017). Plasticity of mitochondrial translation. Trends Cell Biol 27, 712-721.
- Desai N, Brown A, Amunts A, Ramakrishnan V (2017). The structure of the yeast mitochondrial ribosome. Science 355, 528-531.
- Dienhart MK, Stuart RA (2008). The yeast Aac2 protein exists in physical association with the cytochrome bc1-COX supercomplex and the TIM23 machinery. Mol Biol Cell 19, 3934-3943.
- Dujeancourt L, Richter R, Chrzanowska-Lightowlers ZM, Bonnefoy N, Herbert CJ (2013). Interactions between peptidyl tRNA hydrolase homologs and the ribosomal release factor Mrf1 in S. pombe mitochondria. Mitochondrion 13, 871-880.
- Faure S, Higgins J, Turner A, Laurie DA (2007). The FLOWERING LOCUS T-like gene family in barley (Hordeum vulgare). Genetics 176, 599-609.
- Gombault A, Godin F, Sy D, Legrand B, Chautard H, Vallee B, Vovelle F, Benedetti H (2007). Molecular basis of the Tfs1/Ira2 interaction: a combined protein engineering and molecular modelling study. J Mol Biol 374, 604-617
- Greber BJ, Boehringer D, Leibundgut M, Bieri P, Leitner A, Schmitz N, Aebersold R, Ban N (2014). The complete structure of the large subunit of the mammalian mitochondrial ribosome. Nature 515, 283-286.
- Gruschke S, Grone K, Heublein M, Holz S, Israel L, Imhof A, Herrmann JM, Ott M (2010). Proteins at the polypeptide tunnel exit of the yeast mitochondrial ribosome. J Biol Chem 285, 19022-19028.
- Haque ME, Spremulli LL, Fecko CJ (2010). Identification of protein-protein and protein-ribosome interacting regions of the C-terminal tail of human mitochondrial inner membrane protein Oxa1L. J Biol Chem 285, 34991-34998.
- He S, Fox TD (1997). Membrane translocation of mitochondrially coded Cox2p: distinct requirements for export of N and C termini and dependence on the conserved protein Oxa1p. Mol Biol Cell 8, 1449-1460.
- Hell K, Herrmann J, Pratje E, Neupert W, Stuart RA (1997). Oxa1p mediates the export of the N- and C-termini of pCoxII from the mitochondrial matrix to the intermembrane space. FEBS Lett 418, 367-370.
- Hell K, Herrmann JM, Pratje E, Neupert W, Stuart RA (1998). Oxa1p, an essential component of the N-tail protein export machinery in mitochondria. Proc Natl Acad Sci USA 95, 2250-2255.
- Hell K, Neupert W, Stuart RA (2001). Oxa1p acts as a general membrane insertion machinery for proteins encoded by mitochondrial DNA. EMBO J 20, 1281-1288.

- Hoshino S, Kanemura R, Kurita D, Soutome Y, Himeno H, Takaine M, Watanabe M, Nameki N (2021). A stalled-ribosome rescue factor Pth3 is required for mitochondrial translation against antibiotics in Saccharomyces cerevisiae. Commun Biol 4, 300.
- Itoh Y, Andrell J, Choi A, Richter U, Maiti P, Best RB, Barrientos A, Battersby BJ, Amunts A (2021). Mechanism of membrane-tethered mitochondrial protein synthesis. Science 371, 846-849.
- Jia L, Dienhart M, Schramp M, McCauley M, Hell K, Stuart RA (2003). Yeast Oxa1 interacts with mitochondrial ribosomes: the importance of the Cterminal region of Oxa1. EMBO J 22, 6438-6447
- Jia L, Kaur J, Stuart RA (2009). Mapping of the Saccharomyces cerevisiae Oxa1-mitochondrial ribosome interface and identification of MrpL40, a ribosomal protein in close proximity to Oxa1 and critical for oxidative phosphorylation complex assembly. Eukaryot Cell 8, 1792–1802.
- Kummer E, Schubert KN, Schoenhut T, Scaiola A, Ban N (2021). Structural basis of translation termination, rescue, and recycling in mammalian mitochondria. Mol Cell 81, 2566-2582 e2566.
- Mick DU, Fox TD, Rehling P (2011). Inventory control: cytochrome c oxidase assembly regulates mitochondrial translation. Nat Rev Mol Cell Biol 12,
- Mima J, Hayashida M, Fujii T, Narita Y, Hayashi R, Ueda M, Hata Y (2005). Structure of the carboxypeptidase Y inhibitor IC in complex with the cognate proteinase reveals a novel mode of the proteinase-protein inhibitor interaction. J Mol Biol 346, 1323-1334.
- Morgenstern M, Stiller SB, Lubbert P, Peikert CD, Dannenmaier S, Drepper F, Weill U, Hoss P, Feuerstein R, Gebert M, et al. (2017). Definition of a High-Confidence Mitochondrial Proteome at Quantitative Scale. Cell Rep 19, 2836-2852.
- Ott M, Herrmann JM (2010). Co-translational membrane insertion of mitochondrially encoded proteins. Biochim Biophys Acta 1803,
- Richter R, Rorbach J, Pajak A, Smith PM, Wessels HJ, Huynen MA, Smeitink JA, Lightowlers RN, Chrzanowska-Lightowlers ZM (2010). A functional peptidyl-tRNA hydrolase, ICT1, has been recruited into the human mitochondrial ribosome. EMBO J 29, 1116-1125.
- Santos B, Zeng R, Jorge SF, Ferreira-Junior JR, Barrientos A, Barros MH (2022). Functional analyses of mitoribosome 54S subunit devoid of mitochondria-specific protein sequences. Yeast 39, 208-229.
- Serre L, Vallee B, Bureaud N, Schoentgen F, Zelwer C (1998). Crystal structure of the phosphatidylethanolamine-binding protein from bovine brain: a novel structural class of phospholipid-binding proteins. Structure 6, 1255-1265.
- Serre L, Pereira de Jesus K, Zelwer C, Bureaud N, Schoentgen F, Benedetti H (2001). Crystal structures of YBHB and YBCL from Escherichia coli, two bacterial homologues to a Raf kinase inhibitor protein. J Mol Biol 310,
- Shemon AN, Heil GL, Granovsky AE, Clark MM, McElheny D, Chimon A, Rosner MR, Koide S (2010). Characterization of the Raf kinase inhibitory protein (RKIP) binding pocket: NMR-based screening identifies smallmolecule ligands. PLoS One 5, e10479.
- Susila H, Purwestri YA (2023). PEBP Signaling Network in Tubers and Tuberous Root Crops. Plants (Basel) 12.
- Tsoy O, Mushegian A (2022). Florigen and its homologs of FT/CETS/PEBP/ RKIP/YbhB family may be the enzymes of small molecule metabolism: review of the evidence. BMC Plant Biol 22, 56
- Westermann B, Neupert W (2000). Mitochondria-targeted green fluorescent proteins: convenient tools for the study of organelle biogenesis in Saccharomyces cerevisiae. Yeast 16, 1421-1427
- Zeng R, Smith E, Barrientos A (2018). Yeast Mitoribosome Large Subunit Assembly Proceeds by Hierarchical Incorporation of Protein Clusters and Modules on the Inner Membrane. Cell Metab 27, 645-656 e647.